

Pressure Variations Produced at the Ocean Bottom by Hurricanes¹

GARY V. LATHAM, ROCKNE S. ANDERSON, AND MAURICE EWING²

*Lamont Geological Observatory, Columbia University
Palisades, New York 10964*

Low-frequency pressure variations (0.1 to 3 hz) associated with the near passage of six hurricanes have been detected by a deep (5.7 km) ocean bottom hydrophone (OBH) located approximately 260 km northeast of Antigua, British West Indies. Recordings made during one hurricane, Arlene, that passed almost directly over the OBH site in August 1963 have been analyzed in detail. Two principal pressure spectral components are observed: (1) normal microseisms with prominent spectral peaks at periods of 2.8, 4.6, and 10 sec for Arlene, and (2) a shorter-period component with periods between 0.5 and 1.0 sec but usually at 0.9 sec. Maximum microseisms at the OBH occur many hours after peak hurricane winds have passed the point of closest approach to the hydrophone; hence, generation does not take place directly beneath the storm. The onset of normal microseisms from Arlene occurs at about the same time at Guadeloupe and the OBH, and this closely parallels increased regional ocean wave activity. The predominant periods for wind waves and swell from hurricane Arlene are approximately twice the periods of the 2.8- and 4.6-sec microseismic spectral peaks respectively, suggesting that the microseisms are produced by the interaction of ocean waves as described by Longuet-Higgins. The interaction does not take place within the storm itself. The microseismic spectral peak at a period of 10 sec may be produced by the direct action of the 10-sec swell on local shorelines. Maximum amplitudes for the high-frequency pressure component coincide with the time of a hurricane's closest approach to the OBH. Thus, it is concluded that this signal is produced directly beneath a hurricane and may serve as a means of tracking its motion.

INTRODUCTION

In March 1963 an investigation was undertaken to determine the feasibility of using hydrophones located on the ocean bottom for the detection of seismic energy. A hydrophone located approximately 260 km northeast of Antigua, British West Indies, at a depth of 5.7 km, has provided an excellent opportunity to conduct this study.

The hydrophone used in this study is connected by cable to a land-based recording site located on the island of Antigua. A low-frequency amplifier (0.025–1.0 hz) and a drum recorder were installed at the shore end of the cable. The drum speed is 60 mm/min and the duration of a record is 12 hours. Minute marks and hour marks are provided by a clock synchronized with WWV. The over-all system response curve is shown in Figure 1. Several one-hour samples of data were recorded on mag-

netic tape but most of the analysis has been done on the visible recordings.

At least 200 earthquakes have been recorded to the present. Increased signal level from six hurricanes has also been recorded. The hurricane recordings are discussed in this paper.

The primary objectives of this study are:

1. To determine what pressure disturbances are produced at the ocean bottom by a nearby hurricane.
2. To determine whether a hurricane produces the observed pressure variations by direct transfer of energy into the water-solid acoustical system or by first producing water waves that then interact to produce bottom pressure variations.
3. To determine whether the generating region is directly beneath the storm or at some distant location.
4. To determine the mode of propagation of the pressure disturbances.

In addressing ourselves to these questions we are led naturally to the subject of microseisms. The literature on this subject is vast. We shall not attempt to credit other work done in this

¹ Lamont Geological Observatory Contribution 1107.

² Also Department of Geology, Columbia University.

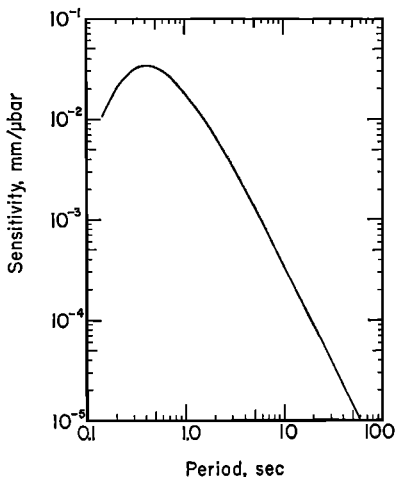


Fig. 1. Over-all response curve for hydrophone and recording system.

area unless it relates directly to the present study.

RECORDING SITE DESCRIPTION

The OBH (ocean bottom hydrophone) location is shown on the maps in Figures 2 and 3. Data on the structure at this site have been obtained by shooting refraction profiles to the hydrophone. A total of 140 shots were fired during two cruises of the Lamont Geological Observatory vessel R. V. *Conrad* in 1963. Details of this work will be reported by R. Houtz et al. (in preparation). The crustal model derived from these profiles is listed in Figure 9. This structure includes a typical oceanic crust, i.e., four principal layers overlying the mantle: water, unconsolidated sediments, basement, and oceanic crust. The regional unconsolidated sediment layer is taken to be 0.31 km thick.

Houtz and Ewing [1964] studied the sediments in the western North Atlantic by means of both refraction and reflection seismic techniques. Their results show that velocity gradients in the sediment layer are variable and are greatest near the water-sediment interface. On the basis of data from 60 profiles they propose the following relation between sediment compressional velocity v and depth h :

$$v = v_0 \left[1 + \frac{kh(n+1)}{v_0 n} \right]^{1/(n+1)} \quad (1)$$

where $n = 5$, $k = 8.75 \text{ sec}^{-1}$, $v_0 = 1.52 \text{ km/sec}$.

For these parameter values (1) becomes

$$v = 1.52(1 + 6.91h)^{1/6} \text{ km/sec} \quad (2)$$

for depth (h) in kilometers.

Accepting this relation as valid for the region near the OBH, we have computed velocity as a function of depth in the sediment. The associated densities and shear velocities have been derived from data given by Nafe and Drake [1963].

For the purposes of computation, the sedimentary column has been arbitrarily divided into four homogeneous layers. The top layer is 0.01 km thick, and each of the three lower layers is 0.1 km thick. The low shear velocities used are consistent with values proposed by Sykes and Oliver [1964a, b] and Oliver and Dorman [1961] to explain short-period oceanic surface waves. The mantle is taken to be a half-space.

AMPLITUDE TIME DEPENDENCE

General description. The tracks of the six hurricanes under study are shown in Figures 2 and 3. These tracks were obtained from U. S. Weather Bureau hurricane tracking charts [*Mariners Weather Log*, 1964, 1965, 1966]. A track represents the path of the center or eye of a hurricane. In considering a hurricane as a source of energy, it must be remembered that strong winds typically extend outward from the eye from 80 to several hundred kilometers. Two of the hurricanes, Arlene and Betsy, were not at full hurricane strength at the time of their closest approach to the OBH. Arlene had degenerated to below hurricane intensity (winds less than 65 knots) approximately 24 hours before her closest approach to the OBH. Regeneration to hurricane intensity did not take place until Arlene had moved 1500 km to the northwest. Betsy had not yet achieved hurricane intensity at the time of her nearest approach to the hydrophone. The four remaining storm systems had all reached hurricane stage before their paths reached the point of minimum distance to the OBH.

As shown in Figure 2, the path of Arlene came nearer to the hydrophone than any of the other hurricanes, passing within 60 km on August 4, 1963. This is the first known case of the recording of low-frequency pressure varia-

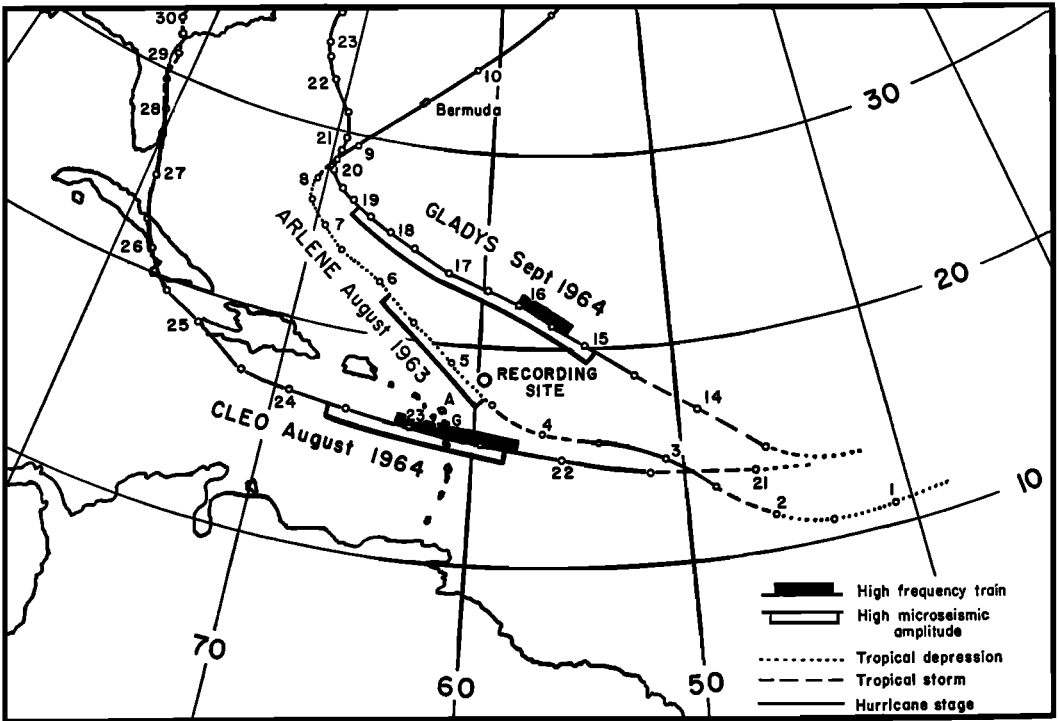


Fig. 2. Tracks of three hurricanes that produced pressure variations at the ocean-bottom hydrophone. Positions are indicated every 12 hours with the date at the 0000 UT position, A, Antigua; G, Guadeloupe.

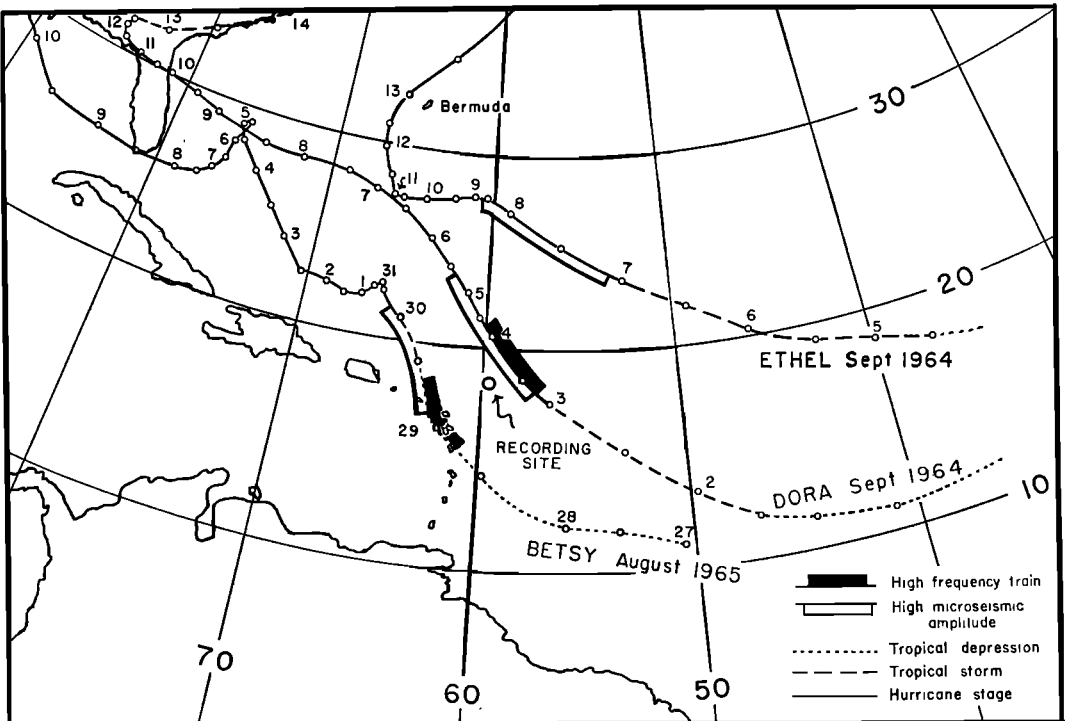


Fig. 3. Tracks of three hurricanes that produced pressure variations at the ocean-bottom hydrophone.

tions on the ocean floor directly beneath a storm of near-hurricane intensity. For this reason, Arlene will be discussed in greater detail than the other hurricanes.

Two principal spectral components are seen by inspection of the records (see Figure 5): a low-frequency component with periods ranging between 2.5 and 6.0 sec and a high-frequency component with periods ranging between 0.5 and 1.0 sec. Time-series analysis reveals greater spectral complexity than this, but for the present we restrict ourselves to the predominant components observed in the records. These two components are discussed separately below.

We shall later identify the low-frequency signals with normal storm microseisms by comparing OBH records with seismograms from a land station. Hence, the low-frequency variations are referred to as microseisms in the following discussion.

Microseisms. The amplitudes and periods of the low-frequency pressure variations were measured visually on the records every 2 hours. In measuring amplitudes, an attempt was made to estimate the peak-to-peak level not exceeded more than 10% of the time. Maximum pressure amplitudes and predominant periods are listed in Table 1. The time interval during which amplitudes exceeded a level equal to 70% of the maximum levels attained during the storm is indicated along the corresponding track for each storm in Figures 2 and 3. From these plots, one point is immediately evident: the distribution of hurricane-generated microseisms at the OBH is not symmetric with respect to the OBH location. Most of the high-amplitude

parts of the microseismic activity plots occurred well after maximum winds had moved beyond the OBH.

It is very difficult to reconcile these observations with a theory that includes generation of microseisms directly beneath the storm. They are easily explained, however, in terms of regional wave action following in the wake of a hurricane as described by *Longuet-Higgins* [1952]. Under this hypothesis, the interval between the time of closest approach of a hurricane to the OBH and the time of peak microseismic activity would be the time required for storm waves to establish an effective interference pattern. The interference may be established directly within the wake of the storm or between waves incident on, and reflected from, the nearest islands of the West Indies arc.

Evidence to support this hypothesis is provided by comparing the amplitude variations of microseisms observed at the hydrophone site with microseisms recorded at Guadeloupe and with regional water wave activity. These comparisons are shown for Arlene in Figure 4.

The seismographs at Guadeloupe are short-period instruments ($T_0 = 1.5$ sec) with peak magnifications of 2000. Amplitude and period readings, made every 3 hours, were kindly supplied to the authors by F. Dorel and M. Feuillard (personal communication, 1964]. Direct wave measurements in the area are not available. Wave forecasts provided by the Fleet Weather Forecasting Office, Suitland, Maryland, can be used, however, for making rough estimates of regional wave activity. This group

TABLE 1. Summary of OBH Hurricane Data

Hurricane	Date of Occurrence	Minimum Distance from OBH, km	Winds at Time of Minimum Distance from OBH, knots	Maximum Pressure Amplitudes ($p - p_0$), μbar		Predominant Periods, sec	
				Microseisms	HF Component	Microseisms	HF Component
Arlene	August 1963	55	25 to 40	850	...	2.5 to 3.0	...
Dora	September 1964	140	100	8200	1000	4.0 to 5.0	0.9
Cleo	August 1964	330	100	830	1000	2.5	0.5 to 0.9
Betsy	August 1965	330	35 to 50	950	250	2.5 to 3.0	0.9
Gladys	September 1964	430	100	2900	400	4.5 to 5.5	0.75 to 1.0
Ethel	September 1964	740	70	3300	...	4.7	...

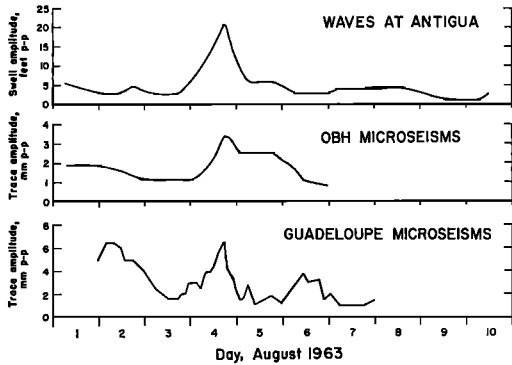


Fig. 4. Amplitude histories of regional water waves (swell) and microseismic amplitudes for hurricane Arlene recorded at Guadeloupe and at the OBH.

produces maps every 6 hours showing the direction, period, and amplitude for both wind waves and swell over the entire North Atlantic Ocean. Average amplitudes and periods for waves in the region between the OBH and the nearest islands of the West Indies arc (Guadeloupe, Antigua, Barbuda) were determined from each map.

At the beginning of the time interval shown in Figure 4, microseismic amplitudes at Guadeloupe and the OBH were decreasing from a previous microseism storm. This microseismic activity appears to be related to the passage of an easterly wave over the island arc (moving westward) during late July and early August. In these latitudes such waves extend northward from weak low-pressure centers located along the equatorial low-pressure trough. There are frequently moderate to heavy showers and thunderstorms to the rear (east) of an easterly wave [Riehl, 1954].

The first noticeable increase in microseismic amplitudes from Arlene is observed in both the Guadeloupe and the OBH records at about 0000 UT, August 4, when the hurricane center was 400 km east-southeast of the OBH and 480 km east of Guadeloupe. The storm at this point was over deep water (5.8 km). Amplitudes increased rapidly to a peak at about 1400 UT, August 4, at Guadeloupe and 1800 UT at the OBH. At the time of peak microseisms at the OBH, the storm center was approximately 80 km west of the OBH with its strong winds moving into shallow water 60 km north

of Barbuda. Amplitudes diminished rapidly at Guadeloupe to near normal at 1200 UT, August 5, but remained high at the OBH until about 0000 UT, August 6. The storm center at this time had moved 800 km northwest of the OBH site. The predominant periods of the microseisms on the Guadeloupe records range between 4 and 5 sec. It is shown in the next section that there are three primary spectral peaks for microseisms from Arlene recorded at the OBH. These peaks occur at 2.7 to 2.9 sec, 4.3 to 5.3 sec, and 10 sec. Thus, microseisms with periods near 5 sec are recorded concurrently at both sites. The short-period microseisms (2.8 sec) are larger than the 5-sec microseisms at the OBH throughout most of the storm. Power spectral density functions were not computed for the Guadeloupe seismograms; consequently, we cannot say whether or not subordinate spectral peaks near periods of 2.8 and 10 sec are also present in the Guadeloupe microseisms. The response of the seismograph at Guadeloupe peaks near 2 sec, however, so that 2.8-sec microseisms would be enhanced on the records relative to 5-sec microseisms. The fact that these shorter-period microseisms are not obvious on the records at Guadeloupe indicates that their relative importance is much less at the island site than at the ocean bottom site.

Ocean wave activity near the islands begins to increase several hours in advance of the onset of increasing microseismic amplitudes at the OBH, but the time of peak wave amplitudes coincides quite closely with the time of peak microseismic amplitudes. Wave periods range between 10 and 14 sec for the swell component and between 4 and 6 sec for the wind wave component.

Despite the fact that the available wave measurements are relatively crude, we believe that the correlation in time between regional water waves and microseisms at the OBH and at Guadeloupe as shown in Figure 4 is sufficient to establish the fact that they are related effects of hurricane Arlene.

Note that, although microseismic amplitudes and ocean wave amplitudes were increasing, the intensity of Arlene was decreasing from a hurricane to a tropical depression. This would appear to support the view that the observed microseisms were produced outside the storm region itself.

High-frequency pressure component. The high-frequency pressure variations mentioned above are observed on the records for four hurricanes. Pertinent data relative to these signals are given in Table 1. A sample of the HF signals, recorded during the later stages of Gladys, is shown in Figure 5. The high-frequency train is superimposed on the longer-period (4.7 sec) microseismic background signal. This train has a period of 0.9 sec and exhibits the very regular, sinusoidal appearance typical of these signals. HF signal amplitudes at the time of this sample had decreased to about one-half of the maximum amplitudes attained during the peak of activity, approximately 7 hours before. In general, as the hurricane approaches the OBH, trains of the type shown in Figure 5 begin to appear every few minutes. The frequency of occurrence, the length of a single train, and the maximum amplitudes increase over a period of hours and then gradually diminish. The buildup and decay are symmetric in time for the HF component as compared with the observed microseismic amplitudes, which have a relatively rapid onset and slow decay.

The total interval over which the HF component is observed for a given hurricane is indicated along the hurricane track in Figures 2 and 3. It is evident from these figures that, to the precision of our measurements, the occurrence of the HF signals is distributed symmetrically with respect to the point of closest approach to the hydrophone for each hurricane. This is in definite contrast to the asymmetric distributions of the low-frequency signals.

It is clear that the high-frequency component

is generated directly beneath, or in the very near vicinity of, the storm system. It is not certain that the high-frequency trains are propagating waves. They may represent standing wave phenomena produced, for example, by interference between ocean waves with periods near 2 sec, or they may be produced by atmospheric pressure variations acting at the water surface. There is no evidence known to the authors that a peak in the ocean wave spectrum of a hurricane exists near 2 sec, or that strong surface pressure variations with a 1-sec periodicity occur within a hurricane. The high-frequency trains are so sinusoidal in appearance and so constant in frequency that a frequency selection process or resonance is suggested. One possibility is that these signals correspond to coupling of acoustic energy into the sediment layer beneath the hydrophone. The fundamental mode corresponding to constructive interference between p waves propagating at nearly vertical incidence within the sediment layer would have a period of 0.74 sec for the assumed sediment thickness of 0.31 km and average velocity of 1.7 km/sec. An increase of assumed sediment thickness to 0.38 km would give the observed period of 0.9 sec for this mode. It should be noted that the high-frequency signals are also produced by local storm activity, so that the mechanism of generation is not related solely to the characteristics of a hurricane. The predominant period and signal character are the same for a local weather system as they are for a hurricane.

The HF component was not observed for hurricane Ethel or Arlene. The absence of this

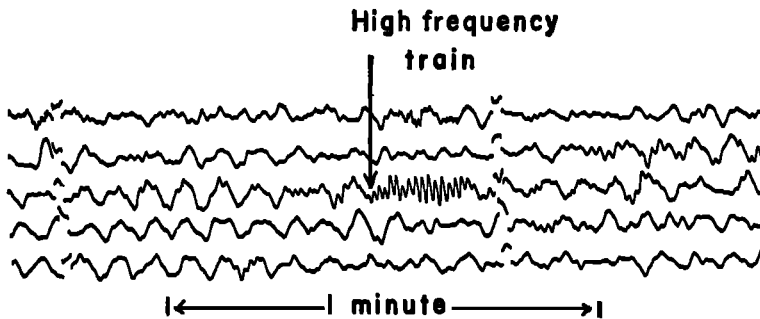


Fig. 5. A sample recording from the ocean-bottom hydrophone showing microseisms of 5-sec period and a HF (high-frequency) train of 0.9-sec period. This recording was made during the late stages of hurricane Gladys, 7 hours after the arrival of maximum amplitudes for the HF component.

component in the case of Arlene is probably explained by the fact that the storm had degenerated to a tropical depression before the time of closest approach to the OBH. Ethel passed at a much greater distance than the other hurricanes and had barely reached hurricane intensity at the time of its closest approach.

PRESSURE POWER SPECTRA

In this section we examine the spectral properties of the microseismic pressure variations from Arlene by means of the power spectral density function. Fifteen data samples were selected for analysis. Each sample is 15 min long with a digitization interval of 0.25 sec and 240 lags (30 degrees of freedom). Computations were carried out following the procedures outlined by *Blackman and Tukey* [1958]. These procedures have been discussed extensively in the literature and will not be discussed in detail in this paper. Raw power density values were smoothed by hamming.

A typical pressure spectrum is shown in Figure 6. Three spectral peaks are prominent at periods of 2.8, 4.8, and 10 sec. Three 1-hour

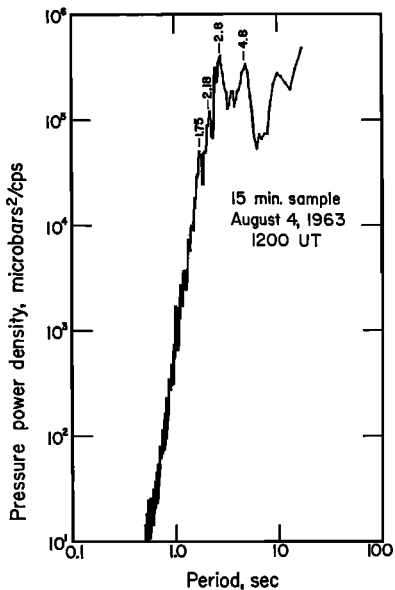


Fig. 6. Pressure power spectral density function for a 15-min sample from the OBH recorded near the time of maximum microseismic amplitudes from hurricane Arlene. Three prominent spectral peaks occur at periods of 2.8, 4.8, and 10 sec.

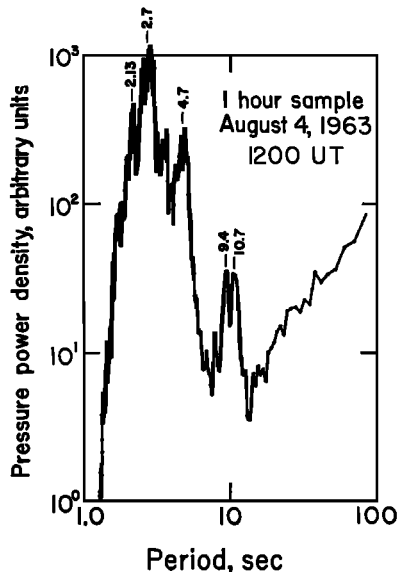


Fig. 7. Pressure power spectral density function for a 1-hour sample from the OBH, recorded near the time of maximum microseismic amplitudes from hurricane Arlene. The spectral peak at the 10-sec period is better defined in this sample. The spectrum is not corrected for instrument response.

samples were analyzed in order to better resolve the long-period end of the spectrum. One of the spectra is shown in Figure 7. Here we see that the peak at 10 sec is actually split into two closely spaced peaks. This feature appears in all the 1-hour samples and may be explained by assuming two separate generating regions at different distances from the storm. Subordinate peaks near 1.8 and 2.1 sec are also present in Figures 6 and 7. In all cases pressure spectral density drops off very rapidly toward the short-period end of the spectrum.

In Figure 8, the fifteen power spectra have been arranged along a time scale and contoured to give a three-dimensional display of the microseismic energy produced by Arlene as the storm passed over the OBH. Dashed lines indicate the periods of the two primary peaks as a function of time. The peak at 10 sec is not well defined on this plot. The following features of this plot are of interest:

1. The period of the intermediate peak varies between 4.3 and 5.3 sec. The short-period peak varies between 2.7 and 2.9 sec.

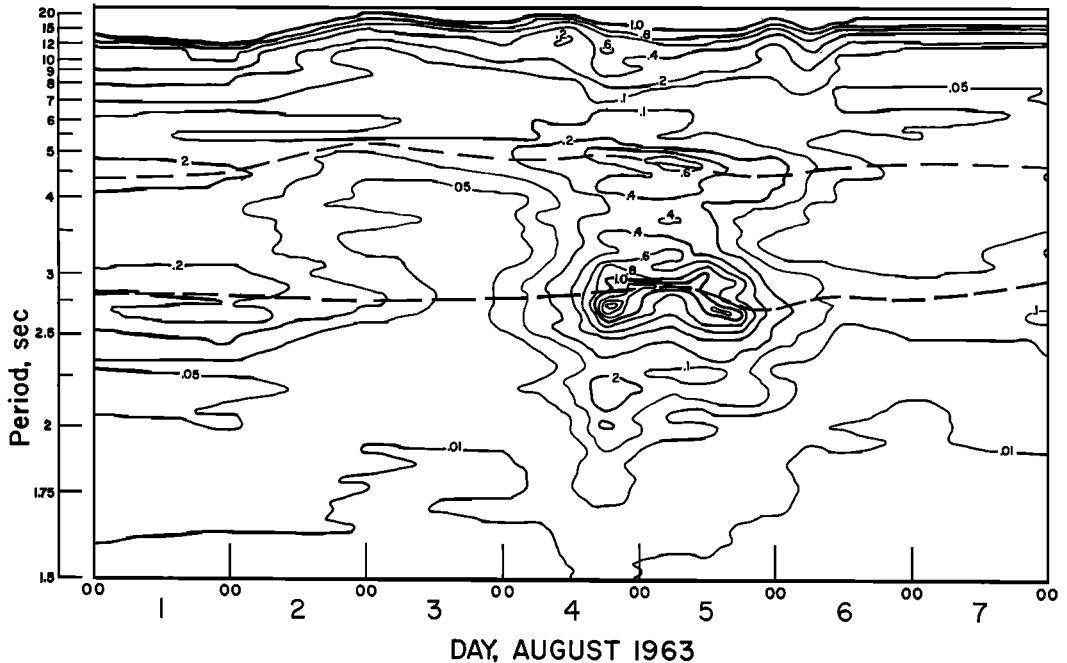


Fig. 8. Contoured plot of pressure spectral density as a function of time during the passage of hurricane Arlene over the ocean bottom hydrophone site. Contour units are millibars²/cps.

2. Microseismic energy associated with the 5-sec peak increases to a maximum at 0600 UT, August 5, and then diminishes to background level during the next 24 hours. As mentioned above, an earlier storm produced the higher contours on the left-hand side of the figure. Energy associated with the short-period peak diminishes from the previous storm to a minimum on August 3 and then builds up rapidly to a maximum at 1800 UT, August 4, and remains at a high level for about 24 hours, before dropping off to near background level again by 1800 UT, August 5. Note that the 5-sec microseisms reach maximum amplitudes approximately 12 hours later than the 2.8-sec microseisms.

3. Some increase in microseismic energy due to Arlene is present throughout the observed part of the spectrum, but most of the increase is confined to the regions near 2.8, 5.0, and 10 sec.

Numerous papers have been written demonstrating the fact that microseisms have either the same period or approximately one-half the period of regional water waves. The papers by *Oliver and Page* [1963], *Haubrich et al.* [1963],

and *Dinger* [1963] are particularly pertinent. *Oliver and Page* show that for large microseismic storms at Palisades, there are two predominant spectral peaks that bear a close 2:1 period relationship to one another throughout the storm. They relate these peaks to storm swell. In the last two papers, the authors compared the spectra of microseisms on land with those of water waves at nearby coastal regions and demonstrated 2:1 and 1:1 period relationships between waves and microseisms. *Latham and Sutton* [1966] showed that microseisms with a 2:1 relationship to both the wind wave and the swell components were present at the ocean bottom near Bermuda.

A theory for the 2:1 period relationship between ocean waves and microseisms waves has been described by *Longuet-Higgins* [1950, 1952]. This theory is based on the effects of nonlinear interaction between opposing water waves of equal or nearly equal period. A theoretical basis for the 1:1 period relationship has been presented by *Hasselmann* [1963]. The basic mechanism in this case is the direct coupling of wave energy into the solid bottom by shoaling action in shallow water.

Based on these studies, we expect that 2:1 and 1:1 period relationships between waves and microseisms should be observed in the present study. This appears to be the case. Based on the wave maps described in the previous section, the period of wind waves near Antigua varied between 4 and 6 sec during Arlene. The period of swell varied between 10 and 14 sec but was usually near 10 sec. This suggests that (1) the microseismic peak near 2.8 sec is produced by wind wave interaction, (2) the microseismic peak near 5 sec is produced by swell wave interaction, and (3) the microseismic peak near 10 sec is produced by direct wave action (swell) in shallow water. The absence of a microseismic component associated with direct wind wave action may be explained by smaller amplitudes of the wind waves compared with swell waves. Also, *Hasselmann* [1963] has shown that the efficiency of microseismic generation by the direct shoaling action of waves increases rapidly with increasing wave period. This factor could explain the generation of observable microseisms by 10-sec waves but not by 4- to 6-sec waves.

As shown in Table 1, the predominant periods of microseisms observed on the records from the more distant hurricanes (Dora, Gladys, and Ethel) are longer than those observed from the nearer hurricanes. Storms at even greater distances, e.g., winter storms in the North Atlantic, produce microseisms at the OBH with periods near 7 sec with no indication of 3-sec microseisms. If the above cause and effect relationship between waves and microseisms is correct, the absence of the shorter-period microseisms from more distant storms is readily explained by the fact that wind waves from these storms would be quite small or nonexistent near Antigua, relative to swell. Similarly, the shift to longer periods for microseisms from distant storms can be explained by the fact that the predominant period of swell increases with increasing distance from the storm region.

OCEAN BOTTOM GROUND AMPLITUDES

In this section, we attempt to determine the ground motion amplitudes at the OBH produced by hurricane Arlene.

Measurements on land [*Toksoz*, 1964; *Douze*, 1964] indicate that most of the energy associated with microseisms propagating across land

masses is in the form of fundamental and higher-mode Rayleigh waves.

Measurements of microseisms on the ocean bottom relating directly to the problem of determining the mode of propagation have been reported by *Schneider and Backus* [1964], *Schneider* [1964], *Schneider et al.* [1964], *Bradner et al.* [1965], and *Latham and Sutton* [1966]. These results are summarized in the paper by Latham and Sutton. The weight of the evidence presented in these papers strongly supports the conclusion that microseisms measured on the ocean bottom are also predominantly Rayleigh waves. *Latham and Sutton* [1966] show that microseisms measured on the ocean bottom near Bermuda are predominantly Rayleigh waves of the fundamental mode. Assuming that the microseisms measured at the OBH from hurricane Arlene are also Rayleigh waves of the fundamental mode, we can compute the particle motion amplitudes corresponding to the observed pressure amplitudes. For the sake of completeness, we have carried out this computation for the first three modes.

It can be shown [*Bradner*, 1962] that for free traveling Rayleigh waves the ratio of pressure to vertical particle velocity at the water-solid interface (at depth H) is given by

$$\frac{P(f)}{\rho_1 \alpha_1 V(f)} = \frac{C_n / \alpha_1}{\left[\left(\frac{C_n}{\alpha_1} \right)^2 - 1 \right]^{1/2}} \cdot \tan \left\{ \frac{2\pi f H}{C_n} \left[\left(\frac{C_n}{\alpha_1} \right)^2 - 1 \right]^{1/2} \right\} e^{i\pi/2}$$

for $C_n > \alpha_1$ (3)

where

$P(f)$ = pressure.

$V(f)$ = vertical particle velocity.

ρ_1, α_1 = density and sound velocity of water.

C_n = phase velocity of n th mode Rayleigh wave.

H = water depth.

f = frequency.

Phase velocities for the first three Rayleigh modes are shown in Figure 9. These curves were derived for the model listed in the figure and discussed in the section on the description of the recording site. Substituting these phase velocity values into (3), we obtain P/V ratios

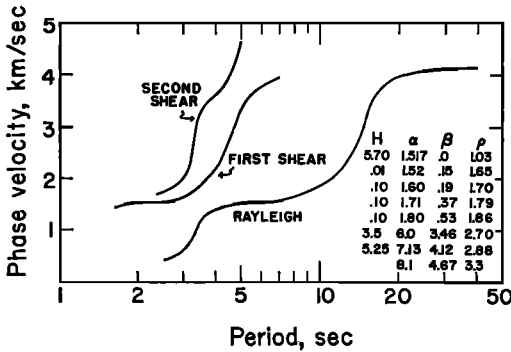


Fig. 9. Theoretical phase velocities for the first three Rayleigh modes for the model taken to represent crustal structure at the OBH site (as listed in the figure).

at the water-sediment interface as shown in Figure 10. Representative values of peak-to-peak pressure measured during the peak of hurricane Arlene are given in Table 2 at periods corresponding to each of the three main spectral peaks. The corresponding amplitudes for Rayleigh particle motion are also listed.

Microseismic amplitudes (vertical component) measured on the ocean bottom near Bermuda were reported to be about 2 microns peak-to-peak [Latham and Sutton, 1966] with an increase to 7 microns during a relatively moderate storm that passed well to the north of Bermuda. Microseisms measured on the ocean bottom 160 km west of San Francisco by the Lamont Geological Observatory Geophysical Station have reached levels of 9 microns during a moderate summer storm in the Gulf of Alaska (A. A. Nowroozi, personal communication, 1966). By comparison with these measurements, the theoretical particle motion amplitudes for Arlene are within the expected range for the fundamental mode. Amplitudes related to the higher modes are also possible, so that propagation in these modes is not ruled out on the basis of data presented in this study alone.

SUMMARY AND CONCLUSIONS

Pressure variations produced at the ocean bottom by a hurricane are of two principal types; normal microseisms with prominent spectral peaks at periods near 2.8, 5, and 10 sec for hurricane Arlene, and high-frequency wave trains with periods between 0.5 and 1.0 sec but usually near 0.9 sec.

Maximum microseismic amplitudes at the OBH (ocean bottom hydrophone) occur many hours after peak hurricane winds have passed the point of closest approach to the hydrophone; hence, generation of microseisms does not take place directly beneath the storm. The onset of increased microseismic amplitudes from Arlene occur at about the same time at Guadeloupe and the OBH, and this closely parallels increased regional wave activity.

The short-period (2.8 sec) microseisms, which are predominant on the records from hurricane Arlene, are absent on records from distant storms. Also, microseisms with the longest periods are related to the most distant storms. This suggests that the shorter-period microseisms are produced by wind waves, and the longer-period microseisms are produced by swell.

The predominant periods for wind wave and swell from hurricane Arlene are approximately twice the periods of the 2.8- and 5-sec microseismic spectral peaks, respectively. This suggests that these microseismic components may be produced by nonlinear wave interaction in the manner described by Longuet-Higgins. The interaction takes place outside the hurricane itself, probably offshore from the nearest islands of the West Indies arc (Antigua, Guadeloupe, and Barbuda). The microseismic spectral peak at 10 sec may be produced by the direct action of the 10-sec swell on local shorelines.

Maximum amplitudes for high-frequency (≈ 1 Hz) pressure variations at the ocean bottom coincide with the time of the storm's

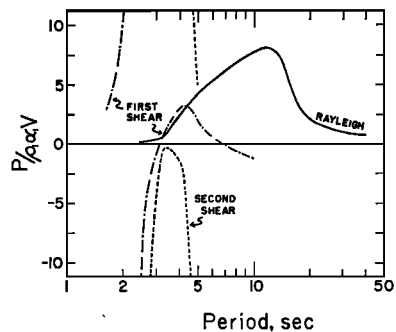


Fig. 10. Ratio of pressure (P) to vertical particle velocity (V) as a function of period for the first three Rayleigh modes represented in Figure 9.

TABLE 2. Pressure Measured on the Ocean Bottom and Calculated Rayleigh Particle Motion Amplitudes for Peak Microseisms from Hurricane Arlene

Period, sec	Pressure Amplitude ($p - p$), μ bar	Ground Motion Amplitude ($p - p$), microns		
		Fundamental Mode	First Shear Mode	Second Shear Mode
2.8	750	61	7.4	1.3
4.8	500	6.1	9.6	2.4
10	500	6.7	36	...

closest approach to the OBH, indicating that this component is generated directly beneath the storm. The mechanism of generation is uncertain.

Microseisms in the period range of 1 to 10 sec exist at the ocean bottom at least 260 km from the nearest land.

Ocean bottom particle motion amplitudes computed from the pressure measurements are in agreement with previous ocean bottom amplitude measurements for Rayleigh waves of the fundamental mode.

Acknowledgments. James Dorman kindly gave us permission to use his surface wave program, PV 7, for computation of Rayleigh wave phase velocities; Maurice Davidson permitted us to use his programs for computation of power spectral density functions. We are also indebted to Leonard Alsop, William Donn, James Dorman, and Paul Pomeroy for critically reviewing the manuscript. Computing facilities were provided by the NASA Goddard Space Flight Center, Institute for Space Studies, New York. The advice and assistance of Gordon Hamilton in many aspects of the program are gratefully acknowledged.

This research was supported by the Advanced Research Projects Agency under the Vela Uniform program through the Office of Naval Research contract Nonr 266 (92).

REFERENCES

- Blackman, R., and J. Tukey, *The Measurement of Power Spectra*, 190 pp., Dover Publications, New York, 1958.
- Bradner, H., Pressure variations accompanying a plane wave propagated along the ocean bottom, *J. Geophys. Res.*, **67**, 3631-3633, 1962.
- Bradner, H., J. Dodds, and R. Foulks, Investigation of microseism sources with ocean-bottom seismometers, *Geophysics*, **30**, 511-526, 1965.
- Dinger, J., Comparison of ocean-wave and microseism spectrums as recorded at Barbados, West Indies, *J. Geophys. Res.*, **68**, 3465-3471, 1963.
- Douze, E., Rayleigh waves in short-period seismic noise, *Bull. Seismol. Soc. Am.*, **54**, 1197-1212, 1964.

- Hasselmann, K., A statistical analysis of the generation of microseisms, *Rev. Geophys.*, **1**, 177-210, 1963.
- Haubrich, R., W. Munk, and F. Snodgrass, Comparative spectra of microseisms and swell, *Bull. Seismol. Soc. Am.*, **53**, 27-37, 1963.
- Houtz, R., and J. Ewing, Sedimentary velocities of the western North Atlantic margin, *Bull. Seismol. Soc. Am.*, **54**, 867-895, 1964.
- Latham, G., and G. Sutton, Seismic measurements on the ocean floor, *J. Geophys. Res.*, **71**, 2545-2572, 1966.
- Longuet-Higgins, M., A theory of the origin of microseisms, *Phil. Trans. Roy. Soc. London*, **A**, **243**, 1-35, 1950.
- Longuet-Higgins, M., Can sea waves cause microseisms?, *Symp. Microseisms, Natl. Acad. Sci. Natl. Res. Council Publ.* **306**, 74-93, 1952.
- Mariners Weather Log*, volumes 8, 9, and 10; 1964, 1965, and 1966.
- Nafe, J., and C. Drake, Physical properties of marine sediments, in *The Sea*, vol. 3, edited by M. N. Hill, pp. 794-815, John Wiley and Sons, New York, 1963.
- Oliver, J., and J. Dorman, On the nature of oceanic seismic surface waves with predominant periods of 6-8 seconds, *Bull. Seismol. Soc. Am.*, **51**, 437-455, 1961.
- Oliver, J., and R. Page, Concurrent storms of long and ultra-long period microseisms, *Bull. Seismol. Soc. Am.*, **53**, 15-26, 1963.
- Riehl, H., *Tropical Meteorology*, pp. 210-234, 392, McGraw-Hill Book Company, Inc., New York, 1954.
- Schneider, W., Ocean-bottom data collection and analysis, *Final Tech. Rept., Contract AF 1Q (604)-8368*, Texas Instruments, Inc., Dallas, Tex., Oct. 1964.
- Schneider, W., and M. Backus, Ocean-bottom seismic measurements off the California coast, *J. Geophys. Res.*, **69**, 1135-1143, 1964.
- Schneider, W., P. Farrell, and R. Brannian, Collection and analysis of Pacific ocean-bottom seismic data, *Geophysics*, **29**, 745-771, 1964.
- Sykes, L., and J. Oliver, The propagation of short-period surface waves across oceanic areas, 1, Theoretical study, *Bull. Seismol. Soc. Am.*, **54**, 1349-1372, 1964a.

Sykes, L., and J. Oliver, The propagation of short-period surface waves across oceanic areas, 2, Analysis of seismograms, *Bull. Seismol. Soc. Am.*, 54, 1373-1415, 1964b.

Toksoz, M., Microseisms and an attempted appli-

cation to exploration, *Geophysics*, 29, 154-177, 1964.

(Received May 4, 1967;
revised June 30, 1967.)